IJPSR (2023), Volume 14, Issue 5 **(Research Article)**

INTERNATIONAL JOURNAL OF PHARMACEUTICAL SCIENCES AND RESEARCH

Received on 05 September 2022; received in revised form, 18 October 2022; accepted 17 November 2022; published 01 May 2023

FORMULATION DEVELOPMENT OF ORAL FAST-DISSOLVING SUBLINGUAL FILM OF RESVERATROL

Vaishali Ashish Shirsat *, Anushree Anil Hukeri and Sneha Balu Govind

Department of Pharmaceutical Analysis, Bombay College of Pharmacy, Kalina, Santacruz East, Mumbai - 400098, Maharashtra, India.

Keywords:

Resveratrol / hydroxypropyl-β-cyclodextrin complex, Kneading method, QbD, fast dissolving film, Sublingual film

Correspondence to Author:
Dr. Vaishali Ashish Shirsat

Associate Professor, Department of Pharmaceutical Analysis, Bombay College of Pharmacy, Kalina, Santacruz East, Mumbai - 400098, Maharashtra, India.

E-mail: vashirsat@gmail.com

ABSTRACT: This research aimed to develop an inclusion complex of resveratrol (RSV)/hydroxypropyl-β-cyclodextrin (HP-β-CD) using a quality-by-design (QbD) approach to improve the solubility and stability of RSV and formulate it into a fast-dissolving sublingual film (FDSF). The RSV/HP-β-CD inclusion complex was prepared by the kneading method using a Box–Behnken Design to assess the effect of the molar ratio of RSV and HP-β-CD, reaction time, and drying time as independent variables on the % entrapment efficiency and % yield. FTIR, DSC, Powder XRD, NMR, and SEM were performed to evaluate the formed complexes. The RSV/HP-β-CD complexation was successful in enhancing RSV solubility and stability. Furthermore, the inclusion complex was incorporated into a fast-dissolving sublingual film. The prepared films were evaluated for a folding endurance test, tensile strength, disintegration time, drug content, thickness, and SEM. The sublingual route of administration was found to be beneficial for films, as it provided 80% permeation of RSV in 60 minutes and no damage to the epithelial tissues was observed in the histopathological study performed on the porcine tongue. Therefore, the developed fast-dissolving sublingual films of the RSV/HP-β-CD inclusion complex were effective for oral administration.

INTRODUCTION: Resveratrol (RSV) is one of the most promising naturally occurring compounds in the polyphenol stilbenoid group, having two phenol rings linked to each other by an ethylene bridge [1, 2, 3]. The chemical structure of RSV (*trans*-3, 5, 4'-trihydroxystilbene) has two structural isomers, *cis*- and *trans*-resveratrol. *Trans*-resveratrol is converted into *cis*-resveratrol in UV rays and *trans*-resveratrol is more stable than *cis*-resveratrol [1, 2, 4].

QUICK RESPONSE CODE

DOI: 10.13040/IJPSR.0975-8232.14(5).2447-66

This article can be accessed online on www.ijpsr.com

DOI link: http://doi.org/10.13040/IJPSR.0975-8232.14(5).2447-66

This natural polyphenol has been detected in more than 70 plant species, especially in grape skin and seeds, and is also found in discrete amounts in red wines and various human foods. It is a phytoalexin that acts against pathogens, including bacteria and fungi [1]. RSV is classified as a BCS class II compound due to its poor aqueous solubility and high permeability [2, 5]. Numerous studies have demonstrated that RSV possesses a very high antioxidant potential as a natural food ingredient.

It also exhibits antitumor activity and is a potential candidate for preventing and treating several types of cancer [1, 6]. Among all these biological properties of RSV, the most useful property of RSV is its capacity to act as a potent antioxidant [7]. RSV antioxidant activity depends upon the arrangement of functional groups on the nuclear structure.

Therefore, the configuration, substitution, and total hydroxyl group number substantially influence several mechanisms of antioxidant activity [8, 9, 10]. RSV is mainly used to minimize or prevent lipid oxidation in pharmaceutical products by delaying toxic oxidation product formation, maintaining both nutritional quality and prolonging pharmaceutical shelflife [11, 12, 13]. Additionally, RSV's antioxidant property helps to protect cells against hydrogen peroxide-induced oxidative stress, whereas pretreatment with resveratrol promotes cell survival and protection against UV irradiation-induced cell death. RSV cellular defense can be achieved by acting as a direct antioxidant and an indirect cellular antioxidant system inducer through modulation of several cellular antioxidant pathways, which helps balance cellular redox status [14, 15, 16].

RSV is a powerful antioxidant, but its clinical applications are strongly limited due to its poor solubility and instability. Due to this poor water solubility, degradation by oxidation and high temperature and light exposure, there is a need to increase the physical stability, chemical stability, and solubility of RSV [6, 17, 18]. Natural and modified cyclodextrin (CD) are effectively used as carriers for water-insoluble drugs, which helps to elevate the solubility and stability of the active pharmaceutical ingredient [19, 20].

Cyclodextrin is a class of cyclic oligosaccharides with hydrophilic outer surfaces and hydrophobic inner cavities. They are classified as α, β and γ cyclodextrin [21]. Some of the modified CDs are methylated beta-cyclodextrin, carboxymethylated beta-cyclodextrin, an amino acid derivative of cyclodextrin, sulfobutyl ether beta-cyclodextrin and hydroxy propyl beta cyclodextrin (HP-β-CD). Each modified cyclodextrin has different binding capacities to the drugs.

There are potentially hundreds or thousands of variations of CDs that have different ring sizes and random or site-specific chemical substitutions. It is believed that the molecular dimensions of the β-CD cavity (diameter 0.60–0.65 nm and height 0.78 nm) make it the ideal host among the three native CDs for inclusion complex formation with most hydrophobic drugs [22, 23]. Drug cyclodextrin inclusion complexes can improve the clinical usage of drugs by increasing their aqueous solubility, dissolution rate, and pharmaceutical availability.

HP-β-CD can be useful to solubilize poorly water-soluble drugs by complexation, and delivery via the sublingual route may increase drug absorption [24]. Many pharmaceutical companies are switching their products from tablets to fast-dissolving films (FDFs). Films have all the advantages of tablets (precise dosage, easy administration) and liquid dosage forms in easy swallowing and rapid bioavailability [25]. Pediatric, geriatric, and bedridden patients or patients with central nervous system dysfunction cannot take regular formulations of tablets and capsules, as they may have difficulty swallowing or chewing. Some patients can have a choking problem. Therefore, FDFs are a better alternative for such cases. This gives the benefit of patient compliance. A fast-dissolving film consists of a very thin oral strip, which is placed on the patient's oral, sublingual mucosal tissue and wetted by saliva; it rapidly hydrates and adheres to the application site and then disintegrates and dissolves to release the medication for oromucosal absorption [26]. The advantages of fast-dissolving sublingual films (FDSFs) are that sublingual delivery of a drug via thin film has the potential to improve the onset of action, lower the dosing and enhance the efficacy and safety profile of the medicament. Compared to orally fast-disintegrating tablets, these films are less friable. A single dose of strip can be carried out individually without requiring the secondary container [27].

In the present study, we prepared RSV/HP-β-CD inclusion complexes using different molar ratios of RSV and HP-β-CD and different reaction times and drying times of the kneading method to determine their effect on the % entrapment efficiency and % yield of the drug by using the QbD approach.

The prepared RSV/HP-β-CD inclusion complex was studied for different characterizations, and a solubility study was carried out to determine the solubility enhancement. The RSV/HP-β-CD inclusion complex was incorporated into fast-dissolving sublingual films and evaluated for various parameters. A permeation study of the prepared film was carried out to check the permeation of the drug *via* the sublingual route, and a histopathological study was performed on the

porcine tongue to determine any harm to the epithelial tissue.

MATERIALS AND METHODS:

Materials: Resveratrol (RSV) was obtained as a gift sample from K. C. Laboratories (Mumbai), and hydroxypropyl-β-cyclodextrin (HP-β-CD) was purchased from Pharmonix Pvt. Ltd. (Thane, India). All other chemicals and solvents were of analytical grade and purchased from S.D. Fine-Chem Limited (Mumbai).

Phase Solubility Studies: A phase solubility study is a quantitative method that measures the solubility of a compound in distilled water. Excess RSV (saturated solution of RSV) was added to polypropylene centrifuge tubes containing distilled water (100mL) and HP-β-CD with increasing molar concentrations (0mM – 20mM). The tubes were shaken in a water shaker bath for 24 hours at 37 °C. Later, the tubes were centrifuged, the supernatant was pipetted out, and the drug concentration was estimated using a UV visible spectrophotometer (Jasco V-630) at λ_{max} 305 nm. The dissolved RSV (mM) concentration was plotted as a function of HP-β-CD concentration (mM).

The apparent 1:1 stability constant (Kc) of RSV and HP-β-CD were calculated based on the slope of the equation and the intrinsic solubility of RSV without HP-β-CD using the following equation:

$$Kc = Slope / S (1 – Slope)$$

Where Kc = Stability constant and S = Solubility of the drug without HP-β-CD (intercept).

Quality by Design (QbD) Approach for Optimization of an Inclusion Complex: Optimizing the inclusion complex was performed using the QbD approach using Design Expert®software, version 11 (DX11). A 3-factor, 3-level Box–Behnken design was used to optimize the formulation variables by running 13 experiments. The independent variables selected were the molar ratio of RSV and HP-β-CD, such as 1:1, 1:2, and 1:3 (A), reaction time (B), and drying period (C). The levels of the independent variables are shown in **Table 1**. The effects of the independent variables on the % entrapment efficiency and % yield were investigated. The analysis of variance (ANOVA) was applied to test the significance and validity of the model.

TABLE 1: INDEPENDENT VARIABLES AND THEIR LEVELS

Independent Variables	Levels		
	Low	Medium	High
	-1	0	+1
Molar ratio of RSV and HP-β-CD	6.74	13.485	20.23
Reaction time (h)	1	1.5	2
Drying period (Days)	2	3	4

Preparation of RSV/HP-β-CD Inclusion Complex:

Kneading Method: The kneading method is one of the more effective methods of inclusion complex preparation. The RSV/HP-β-CD inclusion complex was optimized using a quality-by-design (QbD) approach, which was incorporated into fast-dissolving sublingual films (FDSFs).

The inclusion complex was prepared according to the experimental runs obtained by Design Expert® software by mixing the molar ratio of RSV and HP-β-CD in a mortar with a dropwise addition of ethanol until the formation of a paste and then drying under vacuum to obtain a free-flowing powder. The dried complex was powdered, passed through a BSA 60 mesh sieve and stored in an airtight amber colored container until further use.

Percent Entrapment Efficiency Determination of the RSV/HP-β-CD Inclusion Complex: The percent entrapment efficiency (% EE) was calculated based on the free amount of RSV in the RSV/HP-β-CD inclusion complex. For the determination of % EE, a stock solution was made with an accurately weighed RSV/HP-β-CD inclusion complex containing 10 mg of RSV and diluted to 10 mL with methanol. From this solution, a 10 ppm substock solution was prepared with distilled water, and UV absorbance was recorded at λmax 305 nm.

$$\% EE = A – B / A \times 100$$

Where A = Theoretical amount of RSV in the RSV/HP-β-CD inclusion complex, B = Amount of RSV found in the treated complex

Percent Yield Determination of RSV/HP-β-CD Inclusion Complex: For % yield determination, the prepared complexes were weighed and the yield was calculated. by using the following formula:

% yield = Practical weight of the complex obtained / Theoretical weight of the prepared complex × 100

Statistical Analysis: The data obtained from the QbD trials were analyzed using Design Expert® software, version 11 (Stat-ease Inc., Minneapolis, MN). Several statistical parameters, such as the determination coefficient (R^2), predicted determination coefficient (Predicted R^2), adjusted determination coefficient (Adjusted R^2) and adequate precision, were used to evaluate each model. The P value of analysis of variance (ANOVA) was used to determine the significant effect of a factor on response with a 95% ($p = 0.05$) confidence interval. A P value of less than 0.05 indicates that the model terms are significant, and a value greater than 0.1 indicates the insignificance of the model terms. All these were calculated by using Design Expert®, version 11 software. The three-dimensional response surface plot, two-dimensional counterplot, linearity plot of actual vs. predicted values, and perturbation plot were obtained from Design Expert software to indicate the effect of factor variables on the response variables. These plots were constructed based on the equations obtained from the responses. The optimal inclusion complex was obtained by superimposing the contour plots for each parameter. The model was validated to ensure that the varied input in the same range led to a consistent output in the QbD model for the inclusion complex. The validation of the model was carried out by taking checkpoint batches given by the model within the design range that were not included in the runs given by the software and finding the relative difference between the predicted and observed experimental values.

Characterization of the Optimized RSV/HP-β-CD Inclusion Complex:

Fourier-transform Infrared Spectroscopic Characterization: The infrared spectra of RSV, HP-β-CD, the physical mixture of RSV and HP-β-CD and the RSV/HP-β-CD inclusion complex were obtained using a Jasco Fourier transform infrared spectroscopy (FT-IR)-5300. RSV, HP-β-CD, a physical mixture of RSV and HP-β-CD, and inclusion complex at an amount of 10 mg was mixed with 200 mg of potassium bromide (KBr) and compressed using electrically operated KBr Press model HP-15 and the spectrum was recorded by scanning over a spectral range of 4000-400 cm^{-1} with a resolution of 2 cm^{-1} in the FT-IR spectrophotometer.

Differential Scanning Calorimetry Characterization: Differential scanning calorimetry (DSC) was performed on RSV, HP-β-CD, a physical mixture of RSV and HP-β-CD and the RSV/HP-β-CD inclusion complex using a METTLER TOLEDO instrument to determine the thermal stability of the drug in the formulation. Five milligrams of the sample were weighed and sealed in sample pans. Thermograms were recorded by heating the samples from 30 °C to 300 °C at a heating rate of 10 °C/min under a nitrogen atmosphere with an empty aluminum pan as the reference.

X-ray Diffraction Characterization: The powder X-ray diffraction (PXRD) patterns of RSV, HP-β-CD, the physical mixture of RSV and HP-β-CD and the RSV/HP-β-CD inclusion complex were recorded using a Bruker D8 Discover XRD analyzer (Germany) with Cu-Kα radiation, 40 kV voltage and 30 mA current to determine the crystallinity of the sample before and after complex formulation based on the diffraction angle (θ). The pattern was studied with a scanning range of 10 to 80^0 2θ with a scan speed of 6^0/min.

Nuclear Magnetic Resonance Characterization: The RSV, HP-β-CD, and RSV/HP-β-CD inclusion complexes were studied for nuclear magnetic resonance (NMR) shifts using a Bruker AVANCE 800 plus NMR spectrometer (Mumbai, India). The solvent used for RSV was MeOD (S.D. Fine-Chem Limited (Mumbai), and for the HP-β-CD and RSV/HP-β-CD inclusion complexes, it was D_20 (S.D. Fine-Chem Limited (Mumbai).

Scanning Electron Microscopy Characterization: Scanning electron microscopy **(**SEM**)** analysis of the samples was performed to investigate surface morphology, particle size, and distribution. The morphology of the RSV, HP-β-CD, physical mixture of RSV and HP-β-CD, and

RSV/HP-β-CD inclusion complex were studied using a Carl Zeiss scanning electron microscope (Model No.- Supra 5, Germany). The sample was fixed on an SEM stub using double-sided adhesive tape and then coated with a thin layer of gold, which was operated at 10 kV.

Solubility Study of the RSV/HP-β-CD Inclusion Complex: A saturated solubility study of RSV and the RSV/HP-β-CD inclusion complex was performed to determine the solubility enhancement of RSV in the inclusion complex. Excess amounts of RSV and RSV/HP-β-CD inclusion complexes were dissolved in 5 mL of distilled water individually and sonicated for 10 minutes. The solutions were then shaken for 48 hrs at room temperature and filtered through a 0.45 µm membrane filter. The saturated solubility of RSV in pure RSV and in the RSV/HP-β-CD inclusion complex was measured by using UV spectrophotometry at λmax 305 nm.

Stability Study of the RSV/HP-β-CD Inclusion Complex: The RSV and RSV/HP-β-CD inclusion complexes were studied for stability toward the light, temperature, and humidity. The stability studies were performed for 5 months according to ICH guideline Q1A(R2). Samples were kept in amber-colored bottles at different stations for 5 months. Monthly withdrawal of samples was carried out, and samples were tested for categories such as physical appearance, assay, and solubility. The samples were stored at 5 °C ± 2 °C, 25 °C ± 2 °C/65% RH and 40 °C ± 2 °C/75% RH.

Formulation of fast Dissolving Sublingual Films (FDSFs) of the RSV/HP-β-CD Inclusion Complex:

Preparation of Fast-Dissolving Sublingual Films: The solvent casting method prepared fast-dissolving sublingual films containing RSV/HP-β-CD inclusion complexes. Solution A was prepared by dissolving 30 mg sodium bicarbonate in a beaker containing 10 mL water (to maintain a pH of 8.18 ± 0.05). The optimized inclusion complex equivalent to 200 mg of RSV was dissolved in the above solution by magnetic stirring at 800 rpm to obtain a clear solution, followed by sonication for 15 minutes. The rise in temperature during sonication was prevented by using an ice bath. Solution B was prepared by dissolving 20 mg of sucralose, 5 mg of colorant (FD & C Red No. 3), and 0.2 mL of raspberry as a flavoring agent in 0.5 mL of distilled water. HPMC E6 (1000 mg) was soaked overnight in solution A until it swelled completely and then 0.4 mL PEG 400, 20 mg of poloxamer 407 and 50 mg of carrageenan were added followed by the addition of solution B. The above mixture was then magnetically stirred for approximately 30 minutes at 40 rpm and kept standing overnight to remove entrapped air bubbles. This was then cast on a petri plate and dried in an oven at 50 °C. Once dried, the film was peeled, cut into pieces of 2 x 2 cm area (each containing 20 mg of RSV), wrapped with aluminum foil and stored in a desiccator at 25 °C. The above procedure was carried out by wrapping the apparatus with aluminum foil to prevent exposure of RSV to light since it is a light-sensitive compound.

Evaluation of the Optimized fast Dissolving Sublingual Film (FDSFs):

Folding Endurance Test: The folding endurance was determined by repeatedly folding the films across the same cross-sectional area until the film broke. It is an indicator of the brittleness of the film. Its folding endurance is the number of folding cycles until the film is broken.

Tensile Strength: Tensile strength is the maximum stress applied to a point at which the film breaks. The tensile strength of films was evaluated using a Brookfield CT3^{TM} Texture Analyzer using the dual grip fixture probe. The film was fixed on the holder stage, and a force was applied until the films were separated. Tensile strength was recorded as the maximum force required to separate the film.

The following formula calculates it:

Tensile strength = Maximum load required to break the film (kg) / Original cross-sectional area of the film (cm^2)

Disintegration time: Disintegration time is the time taken for the film to disintegrate when placed sublingually completely. Since it is a fast-dissolving film, quick disintegration of the film was desired. It was determined *in-vitro* by placing the 2 x 2 cm^2 film in a petri plate containing 5-6 mL of simulated saliva (pH 6.8) with intermittent swirling to mimic the *in-vitro* condition of movement of the tongue. The time required for the film to

completely disintegrate is recorded as the disintegration time.

Drug Content and Content Uniformity: The developed HPLC method performed an analysis of the drug content and content uniformity of the film. For drug content determination, a film with dimensions of 2 x 2 $cm^2$was cut and dissolved in an amber-colored volumetric flask using water because the complex between RSV and HP-β-CD could break, and complete analysis of free RSV was possible. A 0.1 mL aliquot was withdrawn and diluted to 10 mL with the mobile phase. The solution was filtered using a 0.22 μm nylon syringe filter and the content was determined by the developed HPLC method.

% drug content= Obtained amount of drug in the film / Loaded amount of drug in the film × 100

The content uniformity was determined by analyzing 5 films cut from different portions. The uniformity in the drug content obtained in all the films was determined by the developed HPLC method.

Moisture Uptake: The test was performed by keeping previously weighed FDSFs strips in a desiccator at 25 °C/65% RH. After 3 days, the strips were removed from the desiccator and reweighed and moisture uptake was calculated.

The following formula calculated the percentage of moisture uptake:

Moisture uptake = Final weight – Initial weight / Initial weight × 100

Thickness of the Film: The thickness of the films was measured using a digital micrometer screw gauge (least count was 0.01 mm). The film was placed between the gauge, and the thickness was measured from 4 different corners of the film and from the center. The average thickness was calculated.

Surface pH Determination: The surface pH of FDSF was determined by slightly wetting the three patches of each formulation with 1 mL distilled water and kept for 30 minutes at room temperature for stabilization. The pH electrode was brought in contact with the film surface and allowed to equilibrate for 1 minute for surface pH measurement.

Scanning Electron Microscopy Characterization: SEM analysis of the samples was performed to investigate the surface morphology, particle size, and size distribution. The morphology of the optimized FDSFs of the RSV/HP-β-CD inclusion complex was determined using a Carl Zeiss scanning electron microscope (Model No- Supra 5, Germany). The films were cut into small pieces, fixed on an SEM stub using double-sided adhesive tape, and then coated with a thin layer of gold, which was operated at 10 kV.

***Ex-vivo* Permeation Study of FDSF:** An *ex-vivo* permeation study was performed through porcine oral mucosa (ventral surface of tongue, procured from Deonar abattoir-Mumbai), and it was carried out using a Franz diffusion cell with an internal diameter of 1.36 cm. The ventral surface of the tongue was excised, trimmed evenly from the sides, washed in isotonic phosphate buffer pH 6.8, and used immediately. The membrane was stabilized before mounting to remove soluble components. It was mounted between the donor and receptor compartments. The donor compartment was filled with a phosphate buffer of pH 6.8, and the receptor compartment was filled with an isotonic phosphate buffer of pH 7.4 at 37 °C ± 2 °C. A 2 x 2 cm film was cut and placed in the donor compartment above the membrane. Hydrodynamics was maintained by stirring with magnetic beads at 50 rpm. 2 mL aliquots were withdrawn from the receptor compartment at predetermined time intervals [0, 5, 10, 15, 20, 25, 30, 45 and 60 minutes], which were replaced with fresh media. The study was performed in triplicate. Drug content was analyzed using the developed HPLC method.

Histopathological Study of FDSF on Porcine Tongue: The anatomy of the porcine tongue is very complex. Any adverse effects or changes in the morphology of the tongue or toxicological reactions due to FDSFs and excipients were studied by histopathological study. A staining technique checked the adverse effect on the porcine tongue after the administration of FDSF. The dorsal and ventral epithelium of the porcine tongue was examined. After the permeation studies, the tongue epithelium tissue was stored in 10% formalin solution (10 mL of formalin was taken in a 100 mL volumetric cylinder and diluted up to 100 mL with phosphate buffer pH 7.4 and stored at room

temperature) at room temperature before pathology examination.

Stability Study of Formulated FDSFs of the RSV/HP-β-CD Inclusion Complex: To check the stability of the developed sublingual film, films were stored by wrapping them in aluminum foil. These were kept in a stability chamber maintained at different temperature conditions: at 4 °C/20% RH, 25 °C/60±5% RH and 40 °C/75±5% RH. The samples were then analyzed in triplicate at specific time periods for 3 months for folding endurance, disintegration time and drug content by the developed HPLC method.

RESULTS AND DISCUSSION:

Phase Solubility Studies: The phase solubility plot of the RSV and HP-β-CD binary systems is shown in **Fig. 1**.

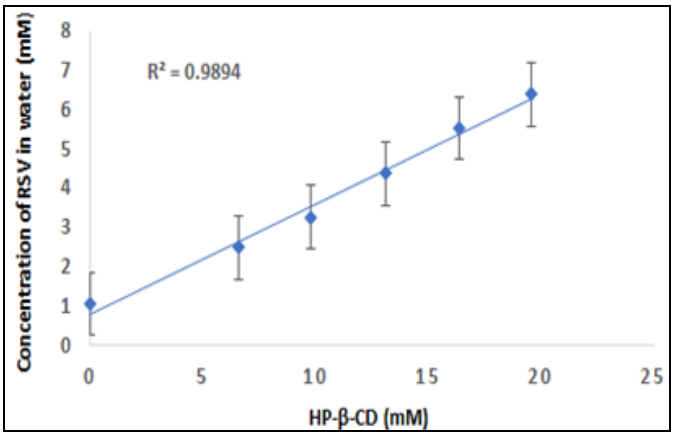

FIG. 1: SOLUBILITY OF RSV IN VARIOUS CONCENTRATIONS OF HP-β-CD

It has been observed from the plot that the aqueous solubility of the RSV drug increased linearly with an increased concentration of HP-β-CD (0 mM – 20 mM).

According to Higuchi and Connors, this type of phase solubility diagram of the drug and HP-β-CD can be considered AL-type. The plot of the drug concentration versus HP-β-CD revealed a straight line with an R^2 of 0.9894 and the slope was calculated to be 0.825. The value of the apparent stability constant (Kc) was found to be 467 M^{-1}, which was in the optimum range of solubility of RSV in water when in contact with HP-β-CD. (20 mM HP-β-CD concentration, the solubility of RSV in water was 14.7 µg/mL at 37 °C).

Box–Behnken Design for Optimization of an Inclusion Complex: The ratio of RSV and HP-β-CD, reaction time, and drying period were optimized using Design Expert software version 11 by the Box Benhken Quality by design (QbD) model. The volume of ethanol and the size of the sieving mesh were fixed during the optimization of the inclusion complex by QbD. The Box–Behnken model consisted of 13 runs based on the limits for the factor variable. The equations proposed by the software for % entrapment efficiency and % yield are as follows:

$$\% \text{ Entrapment efficiency} = 92.00 + 2.06A + 0.6312B + 2.43C - 1.50AB - 0.3750AC - 0.3875BC - 2.13A^2 + 1.63B^2 - 0.7438C^2$$

$$\% \text{ Yield} = 92.30 + 5.06A + 1.25B + 2.87C + 0.0750AB - 0.700AC - 0.5350BC - 3.32A^2 - 0.0550B^2 + 2.22C^2$$

Where A = Molar ratio of RSV and HP-β-CD, B = Reaction time (Hours), C = Drying period (days).

The values of the A, B and C factor coefficients were directly related to the response variables. A positive coefficient indicated a synergistic effect. Its effect is directly proportional to the response and a negative sign indicates an antagonistic effect.

Its effect is inversely proportional to the response. The larger factor coefficients indicate that the causal factor has a more potent influence on the response. The results for the response variables, % entrapment efficiency and % yield are shown in **Table 2**.

TABLE 2: EXPERIMENTAL PLAN AND OBTAINED RESPONSES OF RSV/HP-B-CD INCLUSION COMPLEX

Runs	Factor 1 A: Molar ratio of RSV and HP-β-CD	Factor 2 B: Reaction time (h)	Factor 3 C: Drying period (Days)	Response 1 % Entrapment efficiency	Response 2 % Yield
1	13.485	1	2	89	90.06
2	13.485	1	4	94.25	96
3	13.485	1.5	3	92	92.3
4	13.485	2	2	92.3	94
5	20.23	1.5	2	89	94.8
6	6.74	2	3	91	86

7	20.23	2	3	92	94
8	6.74	1.5	4	90	89
9	20.23	1	3	95	91.7
10	13.485	2	4	96	97.1
11	6.74	1.5	2	84	81
12	6.74	1	3	88	84
13	20.23	1.5	4	93.5	100

Model for % Entrapment Efficiency: The data obtained from the equation of % entrapment efficiency were put into the ANOVA model, and the results are given in **Table 3**. From the results, it was obtained that the Model F value of 11.77 implies that the model was significant. There was only a 3.35% chance that an F value this large could occur due to noise.

A P value less than 0.0500 indicated that the model terms were significant. In the model of % entrapment efficiency, A and C were significant model terms. Values greater than 0.1 indicate the insignificance of the model terms. Adequate Precision measures the signal-to-noise ratio and a ratio greater than 4 is desirable. The adequate precision for the % entrapment efficiency model was 12.694, indicating an adequate signal.

The three-dimensional response surface plot and two-dimensional contour plot were obtained from the data using Design Expert software to indicate the effect of factor variables on the response variables for the % entrapment efficiency model, as shown in **Fig. 2** and **Fig. 3**. The perturbation plot shows the interaction between the factor variables and their effect on the response variable for % entrapment efficiency and the linearity plot showing the actual *vs.* predicted values of % entrapment efficiency is shown in **Fig. 4.**

TABLE 3: ANOVA FOR % ENTRAPMENT EFFICIENCY MODEL

Parameter	Experimental value	Required value
Model F value	11.77	-
P value > F value for model	0.0335	< 0.05
P value > F value for factor A	0.0125	< 0.1
P value > F value for factor B	0.1978	< 0.1
P value > F value for factor C	0.0078	< 0.1
P value > F value for factor AB	0.0696	< 0.1
P value > F value for factor AC	0.5384	< 0.1
P value > F value for factor BC	0.5259	< 0.1
P value > F value for factor A^2	0.0588	< 0.1
P value > F value for factor B^2	0.1072	< 0.1
P value > F value for factor C^2	0.3755	< 0.1
Adjusted R - square	0.8898	-
Predicted R - square	NA	-
Adequate precision	12..694	> 4

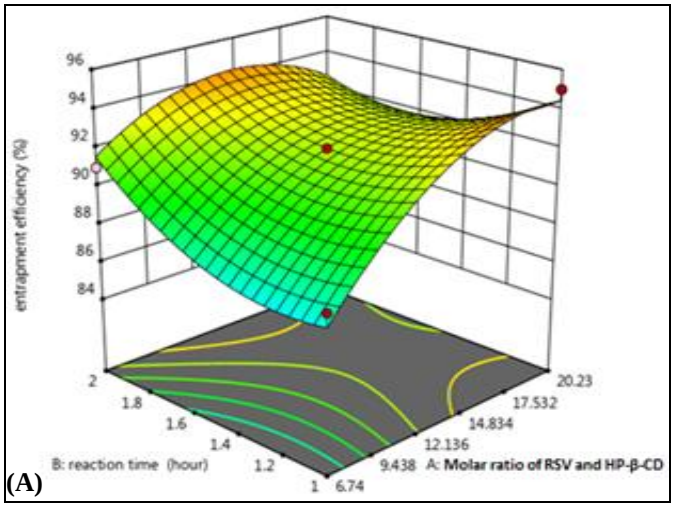

(A)

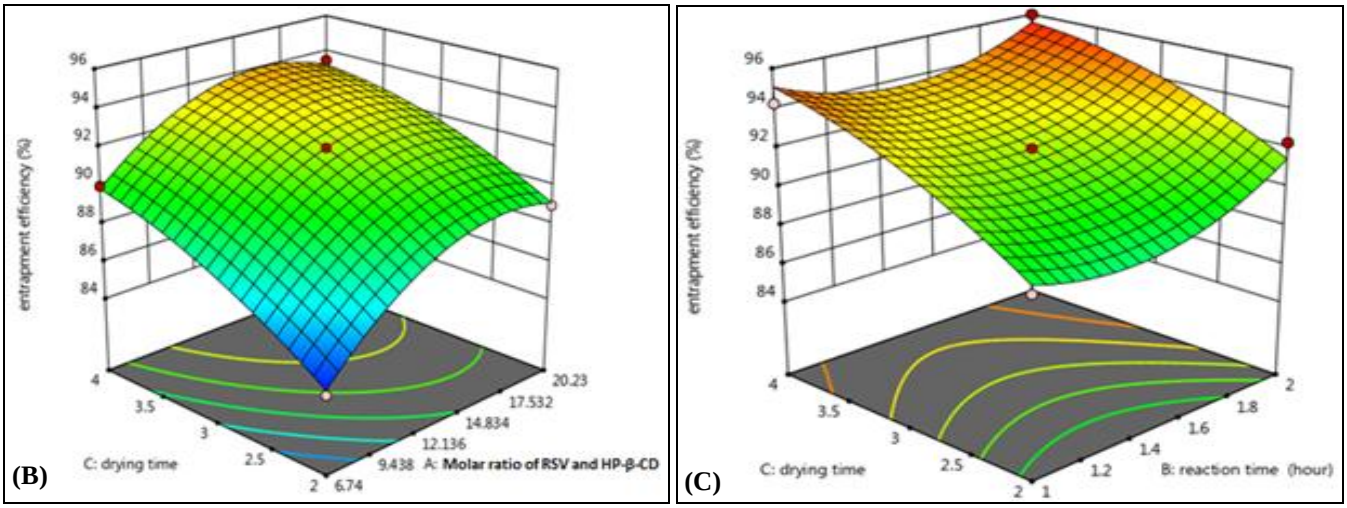

FIG. 2: 3-D RESPONSE SURFACE PLOT SHOWING EFFECT OF (A) MOLAR RATIO OF RSV AND HP-β-CD AND REACTION TIME ON % ENTRAPMENT EFFICIENCY (B) MOLAR RATIO OF RSV AND HP-β-CD AND DRYING TIME ON % ENTRAPMENT EFFICIENCY AND (C) REACTION TIME AND DRYING TIME ON % ENTRAPMENT EFFICIENCY

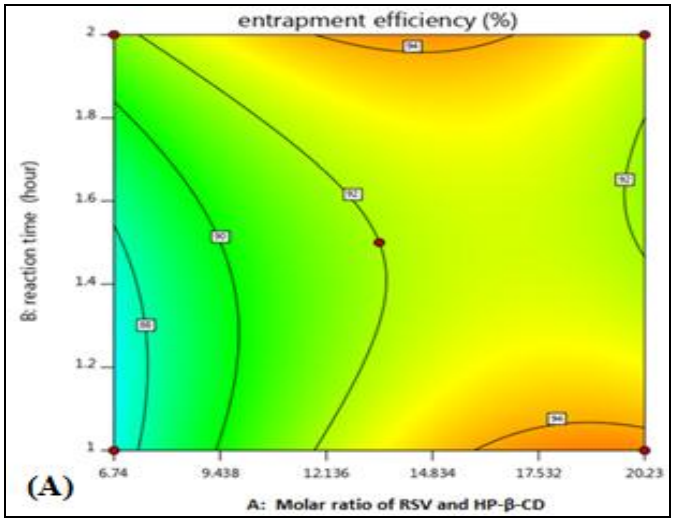

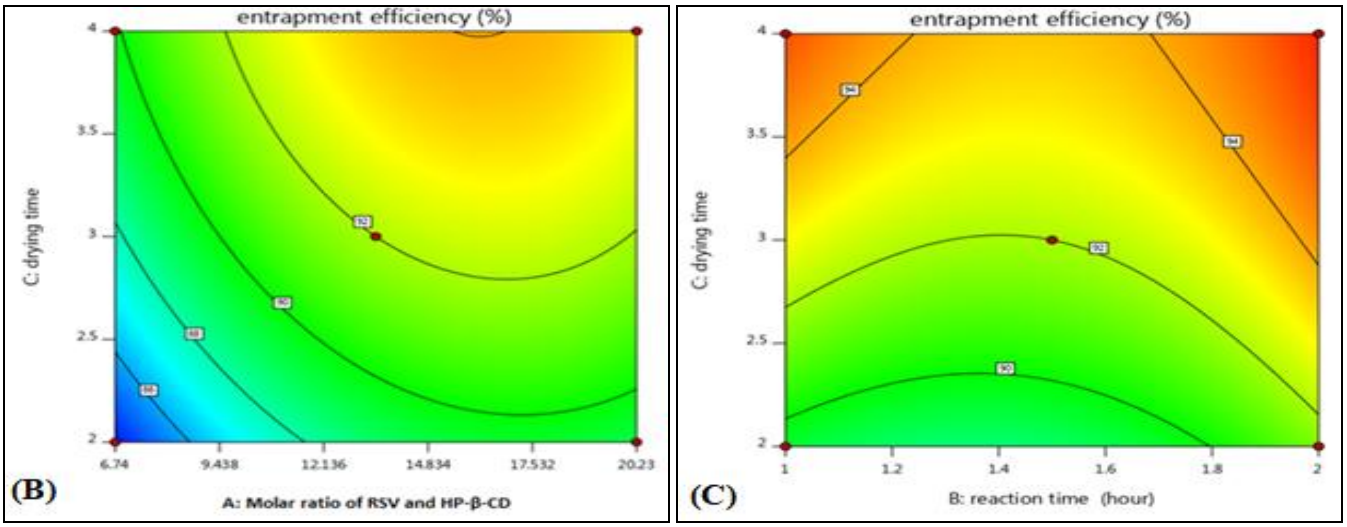

FIG. 3: CONTOUR PLOT SHOWING EFFECT OF (A) MOLAR RATIO OF RSV AND HP-β-CD AND REACTION TIME ON % ENTRAPMENT EFFICIENCY (B) MOLAR RATIO OF RSV AND HP-β-CD AND DRYING TIME ON % ENTRAPMENT EFFICIENCY AND (C) REACTION TIME AND DRYING TIME ON % ENTRAPMENT EFFICIENCY

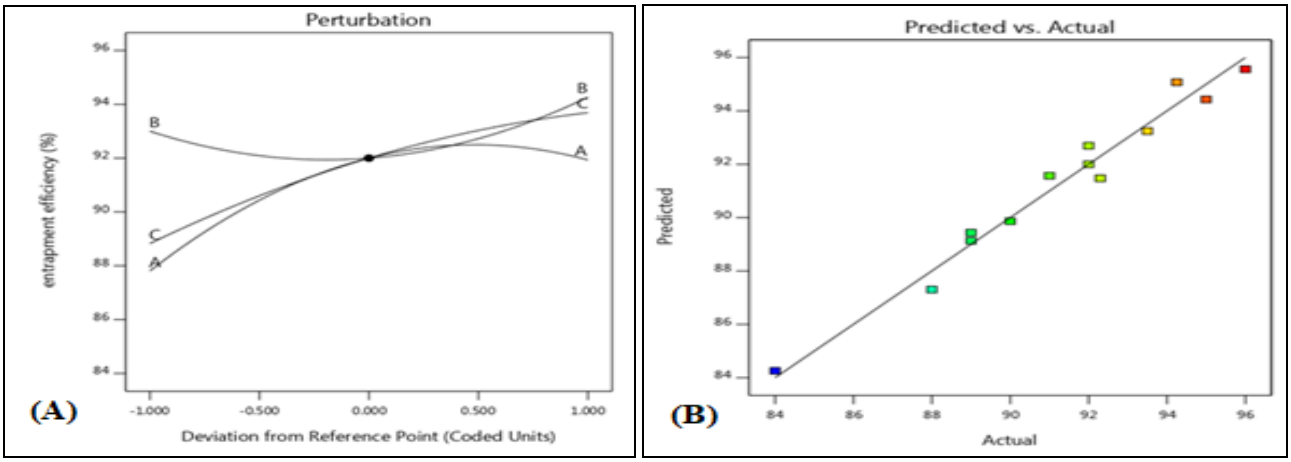

FIG. 4: A) PERTURBATION PLOT SHOWING INTERACTION BETWEEN THE FACTOR VARIABLES AND THEIR EFFECT ON RESPONSE VARIABLE FOR % ENTRAPMENT EFFICIENCY AND B) LINEARITY PLOT SHOWING ACTUAL VS PREDICTED VALUES OF THE % ENTRAPMENT EFFICIENCY

Effect of Factor Variables on % Entrapment Efficiency: An increase in Factor A (molar ratio of RSV and HP-β-CD) led to an increase in the % entrapment efficiency. This increase in the % entrapment efficiency was the logical consequence of the increase in the amount of HP-β-CD since the greater the concentration of HP-β-CD was, the stronger the complex formation.

An increase in Factor B (reaction time) led to an increase in the % entrapment efficiency. This was obtained because more time was available for RSV and HP-β-CD to react in the liquid medium. Factor C (drying time) also showed a proportional effect on % entrapment efficiency.

Validation of the % Entrapment Efficiency Model: The predicted and observed % entrapment efficiency was relatively equal, which indicated minimal % error. The percent error for all checkpoint batches was below 5%. Thus, the design for % entrapment efficiency was validated. Validation data for % entrapment efficiency are given in **Table 4** and a graphical representation of validation data for % entrapment efficiency is shown in **Fig. 5.**

TABLE 4: VALIDATION OF MODEL FOR % ENTRAPMENT EFFICIENCY

Batch no.	Molar ratio of RSV and HP-β-CD	Reaction time (Hours)	Drying period (Days)	Predicted % entrapment efficiency	Observed % entrapment efficiency	% Error
1	11.87	1.5	2.4	89.84	89.8	0.13
2	14.61	1.9	3.0	93.18	93.05	0.14
3	10.75	2.1	3.7	96.03	96.63	0.63

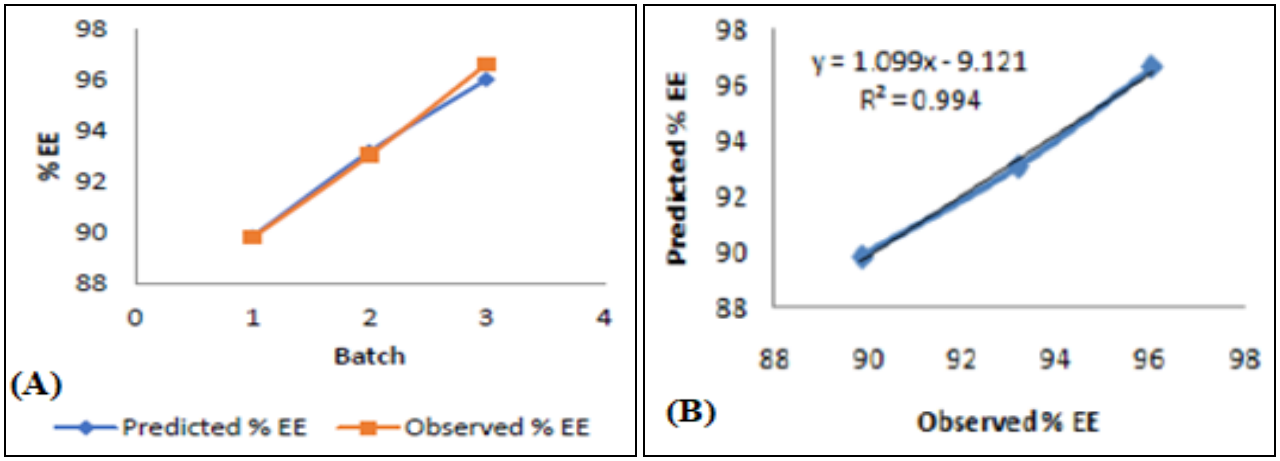

FIG. 5: VALIDATION DESIGN FOR % ENTRAPMENT EFFICIENCY A) PLOT SHOWING PREDICTED AND OBSERVED % ENTRAPMENT EFFICIENCY VS BATCH AND B) OBSERVED VS PREDICTED VALUES OF % ENTRAPMENT EFFICIENCY

Model for % yield: The data obtained from the equation of % yield was put into the ANOVA model, and the results are given in **Table 5**. From the results, it was obtained that the Model F value of 9.873 implies that the model was significant. There was only a 4.04% chance that an F value this large could occur due to noise. AP value less than 0.0500 indicated that the model terms were significant. In the model of % yield, A and C were significant model terms. Values greater than 0.1 indicate the insignificance of the model terms. Adequate Precision measures the signal-to-noise ratio, and a ratio greater than 4 is desirable.

TABLE 5: ANOVA FOR % YIELD MODEL

Parameter	Experimental value	Required value
Model F value	9.873	-
P value > F value for model	0.044	< 0.05
P value > F value for factor A	0.0057	< 0.1
P value > F value for factor B	0.1754	< 0.1
P value > F value for factor C	0.0273	< 0.1
P value > F value for factor AB	0.9452	< 0.1
P value > F value for factor AC	0.5360	< 0.1
P value > F value for factor BC	0.6312	< 0.1
P value > F value for factor A^2	0.0878	< 0.1
P value > F value for factor B^2	0.9696	< 0.1
P value > F value for factor C^2	0.1934	< 0.1
Adjusted R - square	0.8659	-
Predicted R- square	NA	-
Adequate precision	9.873	> 4

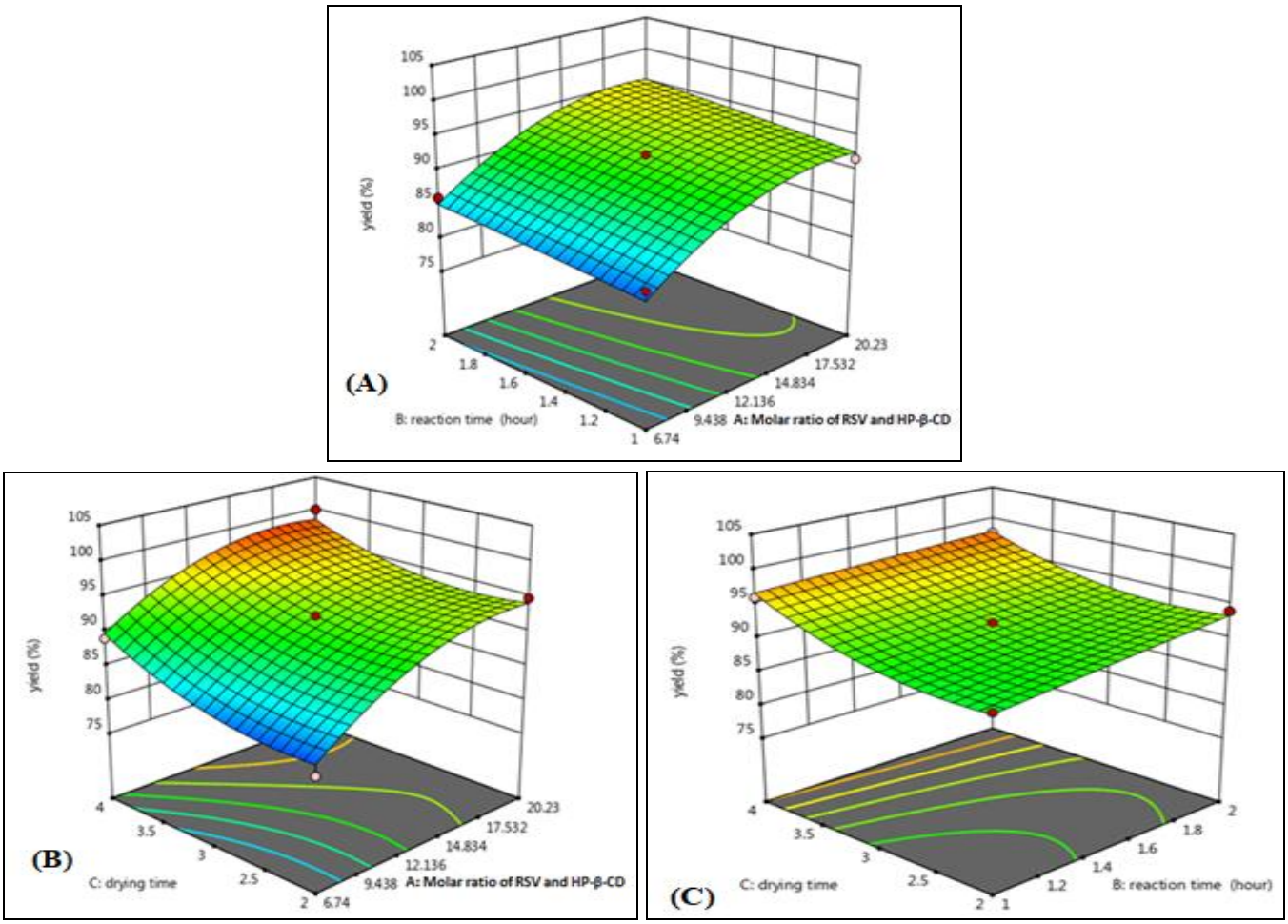

FIG. 6: 3-D RESPONSE SURFACE PLOT SHOWING EFFECT OF (A) MOLAR RATIO OF RSV AND HP-β-CD AND REACTION TIME ON % YIELD (B) MOLAR RATIO OF RSV AND HP-β-CD AND DRYING TIME ON % YIELD AND (C) REACTION TIME AND DRYING TIME ON % YIELD

The adequate precision obtained for the % yield model was 9.873, which indicated an adequate signal. The three-dimensional response surface plot and two-dimensional contour plot were obtained from the data using Design Expert software to indicate the effect of factor variables on the response variables for the % yield model, which is shown in **Fig. 6** and **Fig. 7**. The perturbation plot shows the interaction between the factor variables and their effect on the response variable for % yield and the linearity plot showing the actual vs. predicted values of % yield is shown in **Fig. 8.**

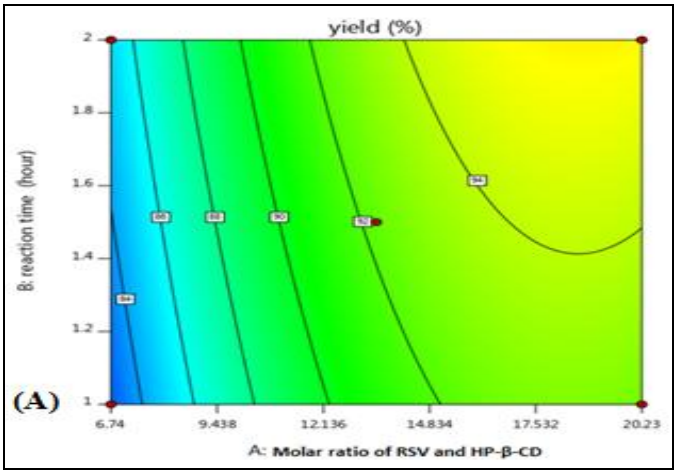

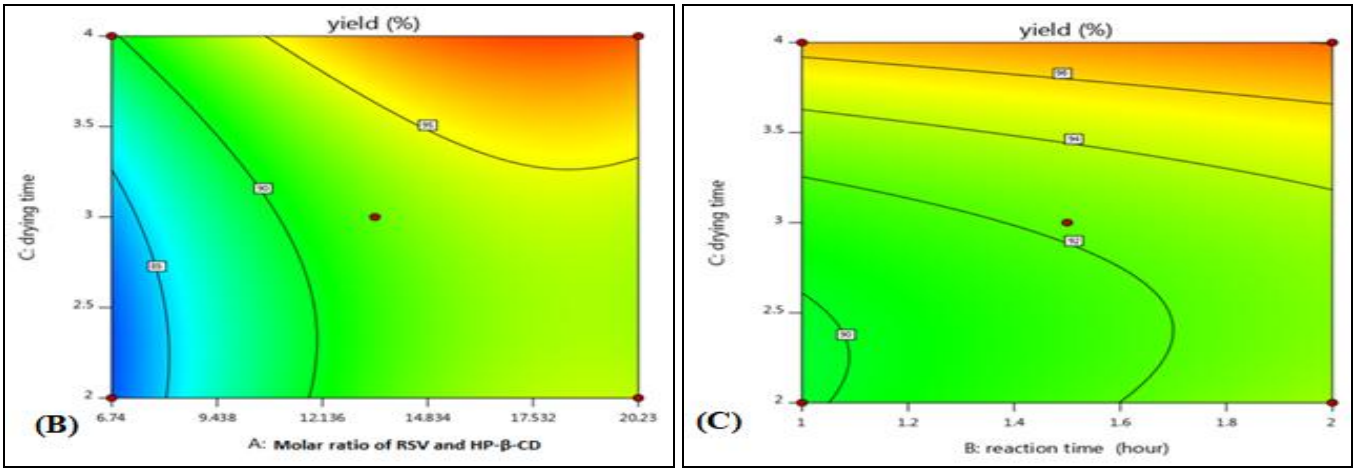

FIG. 7: CONTOUR PLOT SHOWING EFFECT OF (A) MOLAR RATIO OF RSV AND HP-β-CD AND REACTION TIME ON % YIELD (B) MOLAR RATIO OF RSV AND HP-β-CD AND DRYING TIME ON % YIELD AND (C) REACTION TIME AND DRYING TIME ON % YIELD

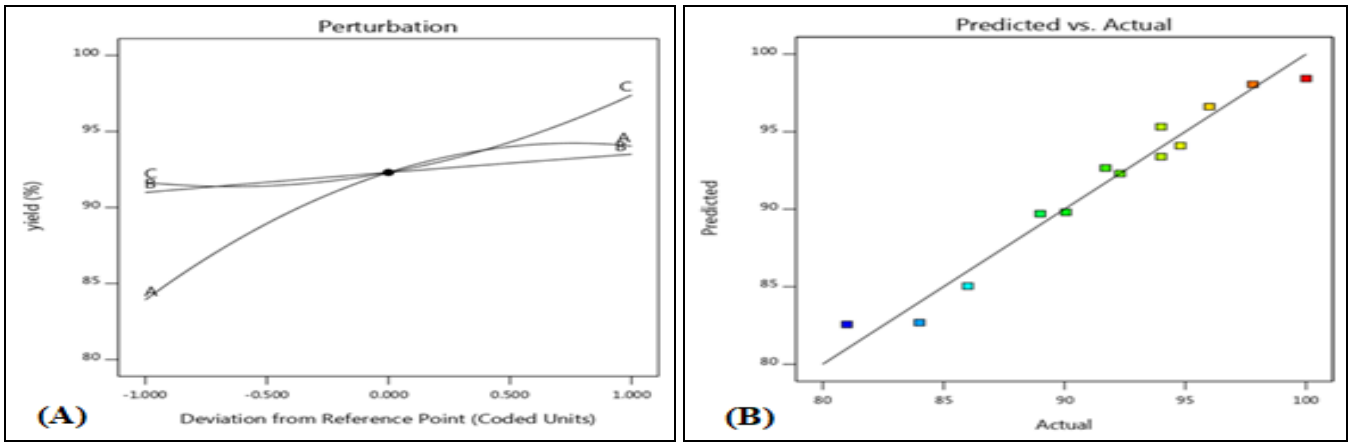

FIG. 8: A) PERTURBATION PLOT SHOWING INTERACTION BETWEEN THE FACTOR VARIABLES AND THEIR EFFECT ON RESPONSE VARIABLE FOR % YIELD AND B) LINEARITY PLOT SHOWING ACTUAL VS PREDICTED VALUES OF THE % YIELD

Effect of Factor Variables on % Yield: An increase in Factor A (molar ratio of RSV and HP-β-CD) led to an increase in % yield. Removal of solvent was a crucial step that gave a paste of RSV and HP-β-CD, resulting in a % yield.

An increase in Factor B (reaction time) has practically no effect on % yield. With an increase in the levels of Factor C (drying time), a slight increase in % yield was found. As the drying time was increased, the more dry amorphous powder was obtained, which affected the % yield of the powder form of the inclusion complex.

Validation of % Yield Model: The results for predicted and observed % yield was relatively equal, which indicated minimal % error. The percent error for all checkpoint batches was below 5%. Thus, the design for % yield was validated. Validation data for % yield is given in **Table 6,** and a graphical representation of validation data for % yield is shown in **Fig. 9.**

TABLE 6: VALIDATION OF MODEL FOR % YIELD

Batch No.	Molar ratio of RSV and HP-β-CD	Reaction time (Hours)	Drying period (Days)	Predicted % yield	Observed % yield	% Error
1	11.87	1.5	2.4	87.18	87.3	0.40
2	10.75	2.1	3.7	94.12	94.24	0.20
3	14.61	1.9	3.0	91.12	90.5	1.18

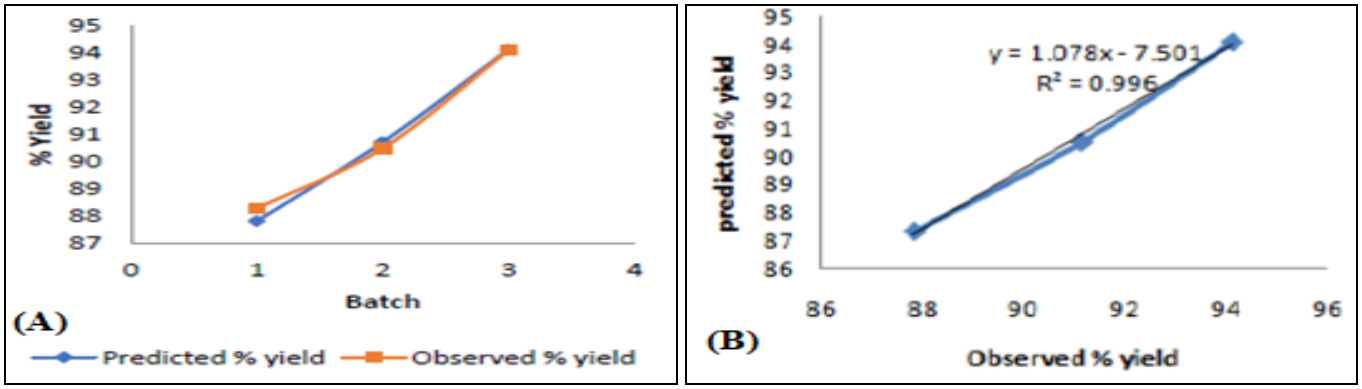

FIG. 9: VALIDATION DESIGN FOR % YIELD A) PLOT SHOWING PREDICTED AND OBSERVED % YIELD VS BATCH AND B) OBSERVED VS PREDICTED VALUES OF % YIELD

Optimized RSV/HP-β-CD Inclusion Complex Obtained by the QbD Approach: From the QbD trials, the final optimized RSV/HP-β-CD inclusion complex was obtained by having a 1:2 molar ratio of RSV and HP-β-CD, 2 hours of reaction time and 4 days as a drying period.

The effect of these optimized independent variables on % entrapment efficiency and % yield was investigated, and it was found that the % entrapment of the optimized inclusion complex was 96%, and the % yield was 97.1%. This optimized RSV/HP-β-CD inclusion complex was further characterized by using different techniques.

Characterization of the Optimized RSV/HP-β-CD Inclusion Complex:

Fourier-transform Infrared Spectroscopic Characterization: The FTIR study was performed to characterize the interaction between RSV and HP-β-CD, and the results are shown in **Fig. 10**. From the FT-IR data, it was observed that all the characteristic peaks of RSV when present in combination with HP-β-CD showed the disappearance of the original peaks of individual RSV, and the appearance of new peaks due to hydrogen bonding was observed. A shift in the wave number was observed. This indicated the complexation of RSV and HP-β-CD.

The FT-IR spectra of the RSV/HP-β-CD inclusion complex **Fig. 10D**. were characterized by 1041 cm^{-1} due to O-H bending, 1590.02 cm^{-1} (C=C), 1561.09 cm^{-1} (C=N stretching), 779.10 cm^{-1} (C-H bending), 845.63 cm^{-1} (N-H bending) and 668.21 cm^{-1} (S-C stretching).

Reduction and extension of C=C characteristic bands (1450–1600 cm^{-1}) confirm the hypothesis that complexation occurs between the aromatic ring within the hydrophobic cavity of HP-β-CD.

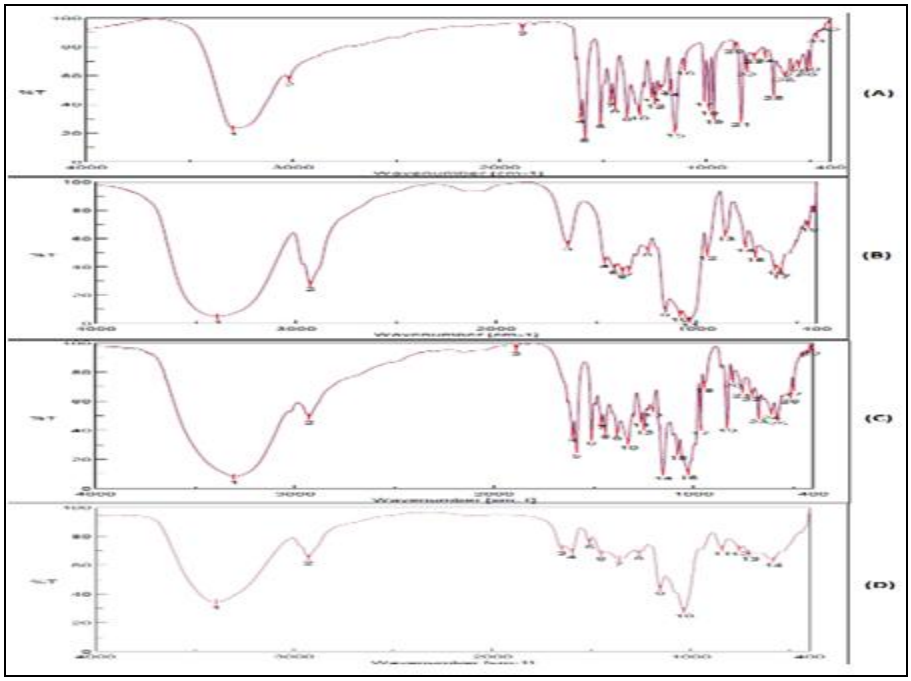

FIG. 10: IR SPECTRA OF (A) RSV (B) HP-β-CD (C) PHYSICAL MIXTURE OF RSV AND HP-β-CD AND (D) RSV/ HP-β-CD INCLUSION COMPLEX

Differential Scanning Calorimetry Characterization: The DSC thermogram of RSV **Fig. 11A** showed an endotherm at 268.67°C corresponding to its melting point. The DSC thermogram of the physical mixture of RSV and HP-β-CD **Fig. 11C** showed endotherms at 99.23°C and 220°C, in which the broadening of peaks indicates water removal. The DSC thermogram of the inclusion complex **Fig. 11**D showed an endothermic peak at 97.81°C. No peak corresponding to the melting point of RSV, i.e., 268.67°C, was observed in the inclusion complex. The disappearance or shifting of the endothermic or exothermic peaks of drugs is mostly an indication of the formation of an inclusion complex and is due to a change in the physical form of RSV from crystalline to amorphous. This indicated that RSV was trapped in the HP-β-CD inner cavity.

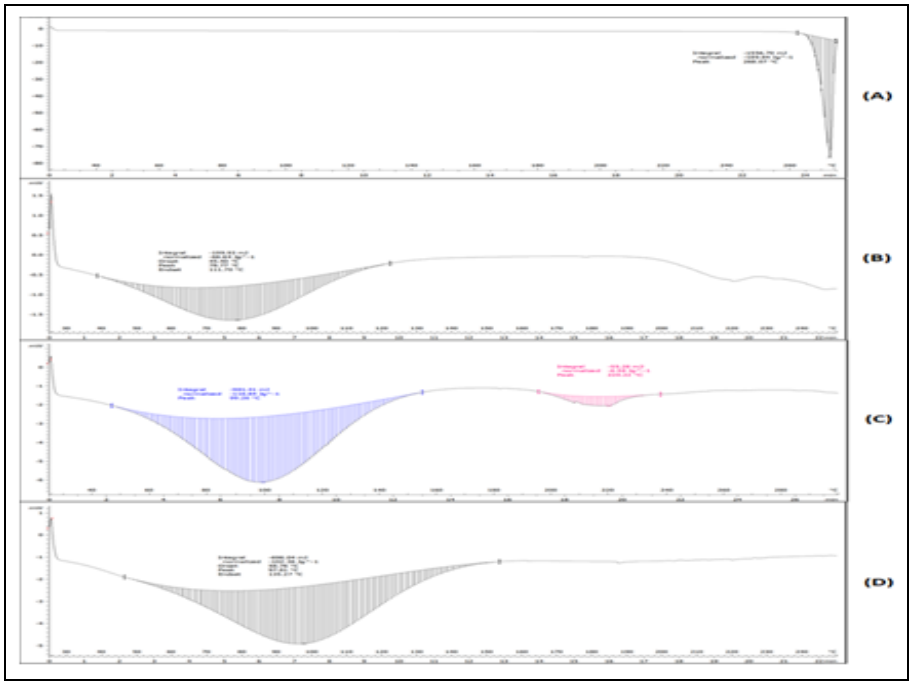

FIG. 11: DSC THERMOGRAM OF (A) RSV (B) HP-β-CD (C) PHYSICAL MIXTURE OF RSV AND HP-β-CD AND (D) RSV/ HP-β-CD INCLUSION COMPLEX

X-ray Diffraction Characterization: PXRD showed the crystallinity of RSV in free form and its amorphous nature after complexation, which confirmed the entrapment of RSV inside HP-β-CD. From the overlay of the XRD spectrum shown in **Fig. 12**, it was observed that in the XRD pattern of RSV **Fig. 12A**, high-intensity peaks were obtained at Θ values of 20^0, 16.5^0, 19^0, 22^0, $24^{0,}$ and $28^{0,}$ indicating the crystalline nature of RSV. In the XRD pattern of the inclusion complex **Fig. 12D**, peaks at 16^0, 19^0, 20^0, 25^0, 28^0 and 15^0 were not observed. This is due to the conversion of the crystalline form of RSV into an amorphous form after entrapment in the cyclodextrin inner cavity. The intensity of the peak at 10^0, $22^{0,}$ and 24^0, 2Θ values were decreased due to the entrapment of the free drug. The occurrence of these 2Θ values in the inclusion complex is due to some of the unentrapped drug present in the inclusion complex.

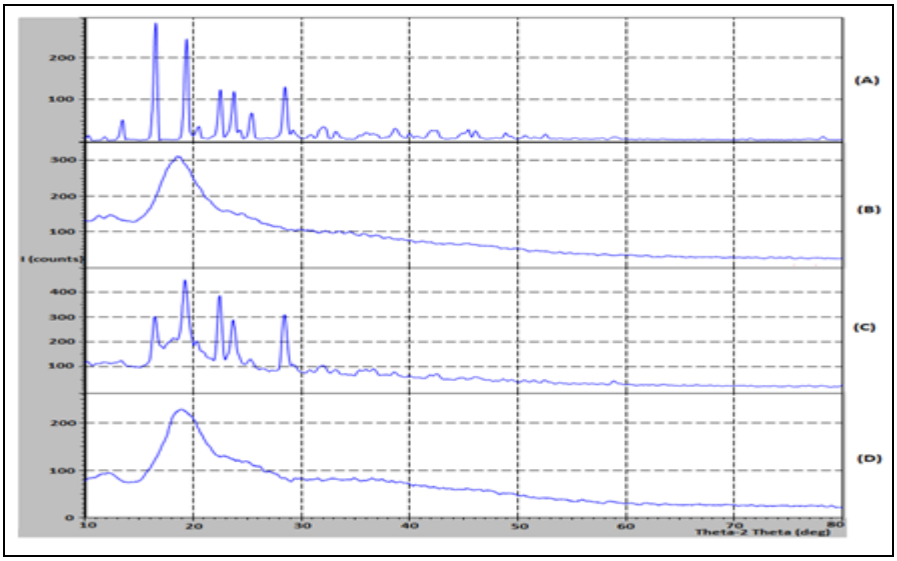

FIG. 12: POWDER XRD GRAPHS OF (A) RSV (B) HP-B-CD (C) PHYSICAL MIXTURE OF RSV AND HP-B-CD AND (D) RSV/ HP-B-CD INCLUSION COMPLEX

Nuclear Magnetic Resonance Characterization: NMR spectra of the RSV/HP-β-CD inclusion complex **Fig. 13C** showed O-H bonding of HP-β-CD and RSV, which confirmed complex formation. The structure of the RSV/HP-β-CD inclusion complex is very complex. Therefore, NMR spectra of RSV **Fig. 13A** and NMR spectra of HP-β-CD **Fig. 13B** were examined. When the NMR spectra of the inclusion complexes were compared with the NMR spectra of RSV, it was observed that the chemical shift values were shifted. This phenomenon indicated complex formation.

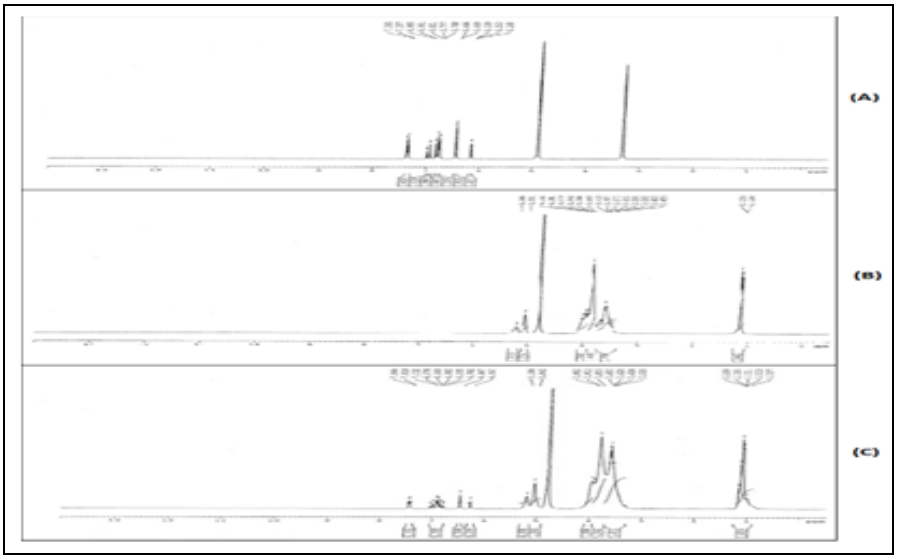

FIG. 13: NMR SPECTRA OF (A) RSV (B) HP-β-CD AND (C) RSV/ HP-β-CD INCLUSION COMPLEX

Scanning Electron Microscopy Characterization: SEM was performed to evaluate the morphology and surface texture of the RSV/HP-β-CD inclusion complex. Scanning electron microscopy was used to determine the surface texture and crystallinity of the samples. SEM images of the RSV standard drug **Fig.14A** showed rod-shaped crystals. Morphology with such a highly crystalline structure led to poor water solubility, poor absorption, and thereby less bioavailability. SEM images of HP-β-CD **Fig. 14B** showed irregularly shaped spheres representing an amorphous nature. SEM images of the physical mixture of RSV and HP-β-CD **Fig. 14C** showed the same properties observed for RSV and HP-β-CD individually. These data conclude that incorporating the drug in the cyclodextrin cavity changes the polymorphic form of the drug from crystalline to amorphous, leading to enhanced water solubility, dissolution, and bioavailability. Hence, RSV/HP-β-CD inclusion complex formation was confirmed by surface texture **Fig. 14D.**

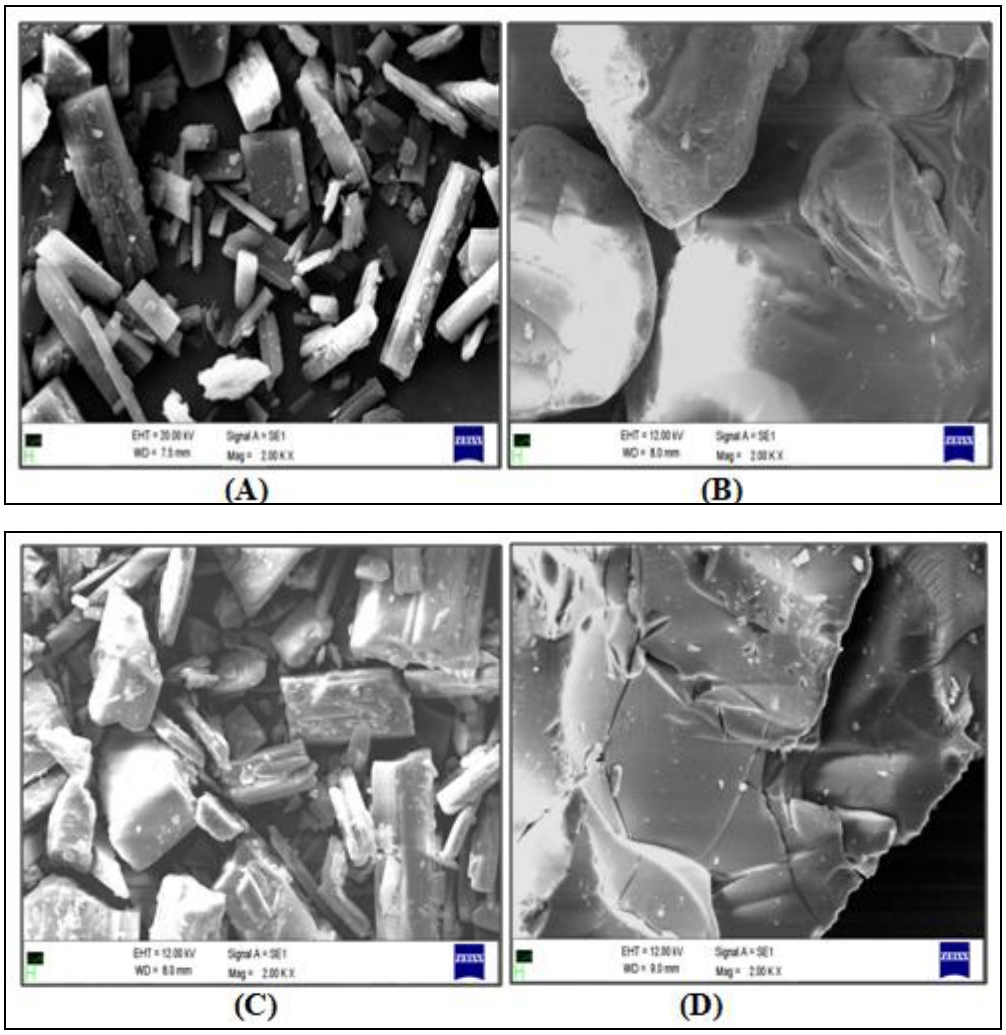

FIG. 14: SEM IMAGES OF (A) RSV (B) HP-B-CD (C) PHYSICAL MIXTURE OF RSV AND HP-B-CD AND (D) RSV/ HP-B-CD INCLUSION COMPLEX

Solubility Study of the RSV/HP-β-CD Inclusion Complex: The solubility of RSV in water was found to be negligible (i.e., 3 mg/100 mL), as very low absorbance in the UV spectra was observed. However, the solubility of the RSV/HP-β-CD inclusion complex in water was found to be 98%, thereby indicating the complexation of RSV and HP-β-CD by increasing the solubility of RSV 90-fold.

Stability Study of the RSV/HP-β-CD Inclusion Complex: Stability studies were performed on three levels, *i.e.*, long-term, accelerated condition and refrigeration for 5 months.

The stability of the RSV drug and RSV/HP-β-CD inclusion complex in solid form was investigated under different storage conditions. When samples were stored at room temperature (25 °C ± 2 °C/65% RH), accelerated temperature (40 °C ± 2 °C/75% RH), and refrigeration temperature (5 °C ± 2 °C), the RSV drug concentration was decreased to 88%, 76% and 94%, respectively, compared with the reference value. Still, the RSV concentration in the complexes was found to be stable, i.e., 97%, 93.87%, and 97.5%, respectively. Thus, the percent level of RSV strongly decreased in the solid state, but the RSV/HP-β-CD inclusion complex was found to be stable under the same storage conditions.

Evaluation of the Optimized Fast Dissolving Sublingual Film (FDSFs):

Folding Endurance: The prepared FDSF did not show any cracks even after folding approximately 300 times, which is a sign of the film's good texture and mechanical properties. Hence, it was taken as the endpoint.

Tensile Strength: The maximum load required to break the prepared FDSF was 3450 gm, and the cross-sectional area was 1600 mm^2. Therefore, the tensile strength required for FDSF was found to be 2.15 $g/mm^{2,}$ which indicates the good strength of the film. **Fig. 15** shows the tensile strength graph of the FDSF.

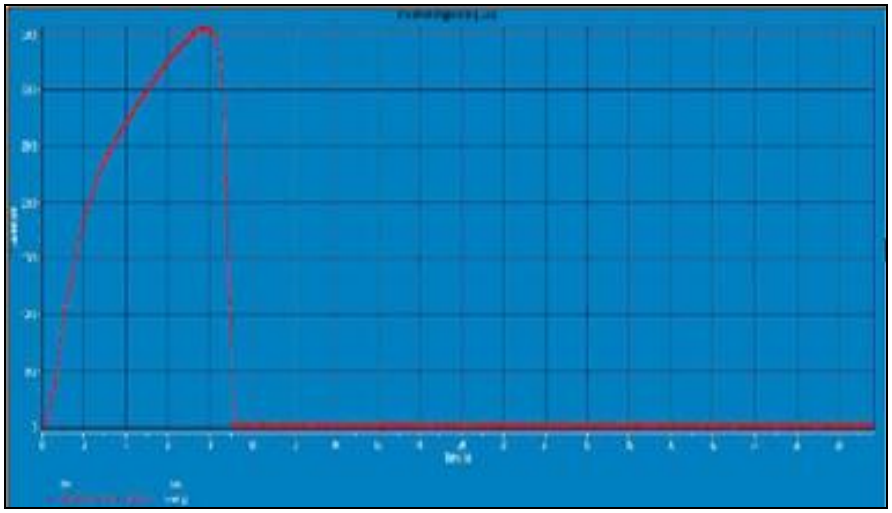

FIG. 15: TENSILE STRENGTH GRAPH OF THE FDSF DISPLAYING THE LOAD (G) REQUIRED TO BREAK THE FILM VS DISTANCE TRAVELLED BY THE FILM (CM) UNTIL IT BREAKS

Disintegration Time: The prepared FDSF was completely disintegrated within < 30 seconds. This was enough time to show a rapid disintegration time when the film was placed in the mouth, reflecting the very short time required for the release of RSV.

Drug Content and Content Uniformity: The drug content of the prepared FDSF was found to be 99%, which indicates good loading of RSV in the prepared films and the drug uniformity of FDSF was also found to be good.

Moisture Uptake: No moisture uptake was observed in the prepared FDSF, which shows that the film has good properties.

Thickness of the Film: The prepared FDSF was found to be 0.1056 ± 0.0017 mm, indicating that the prepared film of suitable thickness can be placed sublingually with no patient inconvenience.

Surface pH Determination: The pH of FDSF in water was found to be 6.79, which is similar to the pH kept during the formulation of FDSF. This indicates that the pH of the film does not change.

Scanning Electron Microscopy Characterization: SEM images of RSV/HP-β-CD inclusion complex-loaded FDSF showed uniformly dispersed particles throughout the film.

Blank film appeared to be loaded with powder because of HPMC addition **Fig. 16** represents the difference in surface texture between the blank film and RSV/HP-β-CD inclusion complex-loaded FDSF.

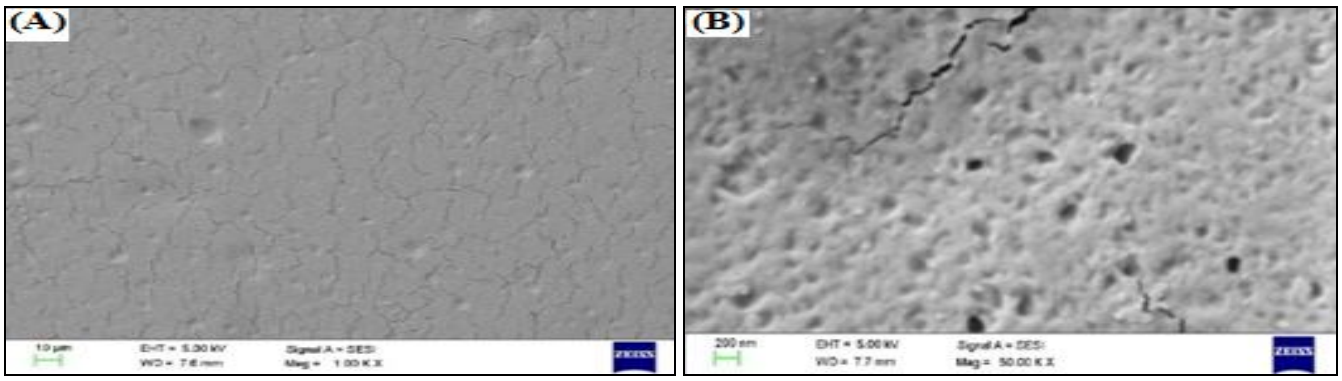

FIG. 16: SEM IMAGES OF (A) BLANK FDSF AND (B) RSV/ HP-β-CD INCLUSION COMPLEX LOADED FDSF

***Ex-vivo* Permeation Study of FDSF:** An *ex-vivo* permeation study helped evaluate the drug's extent of permeation. Drug permeation was studied using two routes of administration, i.e., supralingual and sublingual. The lingual route of administration provided only 20% permeation of RSV in 60 minutes, whereas the sublingual route of administration was found to be beneficial, as it provided 80% permeation of RSV in 60 minutes. The percent cumulative permeation for both routes was plotted at various time intervals, as shown in **Fig. 17**. Thus, the *ex-vivo* study indicated that the drug has a better ability to cross the sublingual barrier faster.

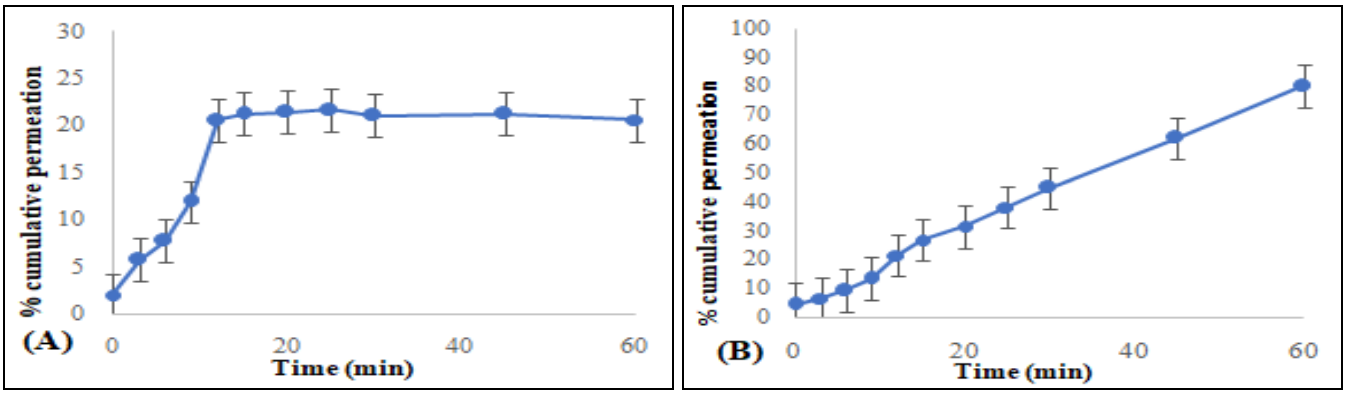

FIG. 17: *EX-VIVO* PERMEATION STUDY OF FDSF BY A) SUPRALINGUAL ROUTE AND B) SUBLINGUAL ROUTE

Histopathological Study of FDSF on Porcine Tongue: The examined section of stratified squamous epithelium of porcine tongue showed normal histological appearance. As shown in **Fig. 18**, there was no damage to the epithelial tissues before and after administration of FDSF, no abnormalities were detected, and the mucosa showed stratified squamous epithelium integrity, which was well maintained. Histological details of the epithelial cells, cytoplasm and nuclei were healthy. No degenerative and/or necrotic changes were noted.

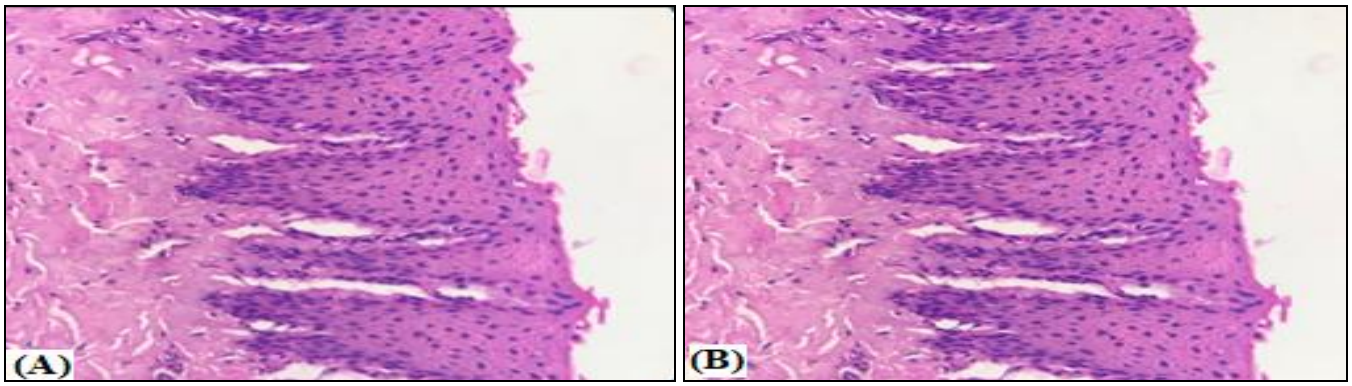

FIG. 18: SECTION OF STRATIFIED SQUAMOUS EPITHELIUM OF PORCINE TONGUE A) WITHOUT ADMINISTRATION OF FDSF B) AFTER ADMINISTRATION OF FDSF

Stability Study of Formulated FDSFs of the RSV/HP-β-CD Inclusion Complex: The data analysis for FDSFs during and after stability studies up to 3 months indicates that the drug molecule RSV remained unchanged in the films and showed no degradation. The % drug content in the 0, 1st, 2nd and 3rd month analyses was within 97–99%. The folding endurance and disintegration time of the optimized films in the subsequent 3 months were the same. Thus, the optimized film was found to be stable for up to 3 months.

CONCLUSION: The goal of the research was to increase the water solubility and stability of the hydrophobic drug resveratrol by incorporating the drug into the hydrophilic cavity of cyclodextrin. Hydroxypropyl-β-cyclodextrin was found to be a perfect modified beta-cyclodextrin for the preparation of an inclusion complex. The inclusion complex of RSV/HP-β-CD was successfully prepared by using the kneading method with the help of the QbD approach. The prepared inclusion complex was found to be stable and improved the solubility of resveratrol.

The RSV/HP-β-CD inclusion complex was incorporated into a fast-dissolving sublingual film, and the film showed 82% drug permeation when administered through the sublingual route. Histopathology of the porcine tongue showed no interaction with the epithelial tissues. Therefore, this RSV/HP-β-CD loaded fast dissolving sublingual film would be a promising and convenient drug delivery system having antioxidant activity.

ACKNOWLEDGMENT: The authors are thankful to the Department of Science and Technology (Ministry of Science and Technology), Government of India, and the Indian Pharmaceutical Association, Maharashtra State Branch, for providing research funds to perform this work under the project entitled “National Facility for Research and Training in Integrated Analytical Strategies for Discovery, Development and Testing of Drugs, Pharmaceuticals and Nutraceuticals” DPRP scheme to Bombay College of Pharmacy, Mumbai, Project Sanction Order no. VI-D&P/552/2016–17/TDT(G), dated 07.03.2017.

CONFLICTS OF INTEREST: The authors declare that there are no conflicts of interest.

REFERENCES:

1. Salehi B, Mishra AP, Nigam M,Sener B, Kilic M, Sharifi-Rad M, Fokou PVT, Martins N and Sharifi-Rad J: Resveratrol: A double-edged sword in health benefits. Biomedicines 2018; 6(3): 91.
2. Peng RM, Lin GR, Ting Y and Hu JY: Oral delivery system enhanced the bioavailability of stilbenes: Resveratrol and pterostilbene. BioFactors 2018; 44(1): 5-15.
3. Lim YR, Preshaw PM, Lin H and Tan KS: Resveratrol and its analogs as functional foods in periodontal disease management. Frontiers in Dental Medicine 2021; 2: 636423.
4. Leri M, Scuto M, Ontario ML, Calabrese V, Calabrese EJ, Bucciantini M and Stefani M: Healthy effects of plant polyphenols: molecular mechanisms. International Journal of Molecular Sciences 2020; 21(4): 1250.
5. Truzzi F, Tibaldi C, Zhang Y, Dinelli G and D′ Amen E: An overview on dietary polyphenols and their biopharmaceutical classification system (BCS). International J of Molecular Sciences 2021; 22(11): 5514.
6. Kim SM and Kim SZ: Biological activities of resveratrol against cancer. Journal of Physical Chemistry & J Biophysics 2018; 8(2): 267.
7. Meng T, Xiao D, Muhammed A, Deng J, Chen L and He J: Anti-inflammatory action and mechanisms of resveratrol. Molecules 2021; 26(1): 229.
8. Li QS, Li Y, Deora GS and Ruan BF: Derivatives and analogues of resveratrol: recent advances in structural modification. Mini Reviews in Medicinal Chemistry 2019; 19(10): 809-25.
9. Li Z, Chen X, Liu G, Li J, Zhang J, Cao Y and Miao J: Antioxidant activity and mechanism of resveratrol and polydatin isolated from mulberry (*Morus alba* L.). Molecules 2021; 26(24): 7574.
10. Silva AF, Monteiro M, Resende D, Braga SS, Coimbra MA, Silva AM and Cardoso SM: Inclusion Complex of Resveratrol with γ-Cyclodextrin as a Functional Ingredient for Lemon Juices. Foods 2020; 10(1): 16.
11. Colica C, Milanović M, Milić N, Aiello V, De Lorenzo A and Abenavoli L: A systematic review on natural antioxidant properties of resveratrol. Natural product communications 2018; 13(9): 1195-1203.
12. Papuc C, Goran GV, Predescu CN, Nicorescu V and Stefan G: Plant polyphenols as antioxidant and antibacterial agents for shelf-life extension of meat and meat products: Classification, structures, sources, and action mechanisms. Comprehensive Reviews in Food Science and Food Safety 2017; 16(6): 1243-1268.
13. Gonzalez-Freire M, Diaz-Ruiz A, Hauser D, Martinez-Romero J, Ferrucci L, Bernier M and de Cabo R: The road ahead for health and lifespan interventions. Ageing research reviews 2020; 59: 101037.
14. Means JC, Gerdes BC and Koulen P: Distinct mechanisms underlying resveratrol-mediated protection from types of cellular stress in C6 glioma cells. International journal of molecular sciences 2017; 18(7): 1521.
15. Zhang X, Liu X, Wan F, You W, Tan X, Sheng Q, Li C, Hu Z, Liu G and Zhao H: Protective effect of resveratrol against hydrogen peroxide-induced oxidative stress in bovine skeletal muscle cells. Meat Science 2022; 185: 108724.
16. Kumar S, Chang YC, Lai KH and Hwang TL: Resveratrol, a molecule with anti-inflammatory and anti-cancer activities: natural product to chemical synthesis. Current Medicinal Chemistry 2021; 28(19): 3773-86.

17. De Vries K, Strydom M and Steenkamp V: Bioavailability of resveratrol: Possibilities for enhancement. Journal of Herbal Medicine 2018; 11: 71-7.
18. Cheng JG, Tian BR, Huang Q, Ge HR and Wang ZZ: Resveratrol functionalized carboxymethyl-β-cyclodextrin: synthesis, characterization, and photostability. Journal of Chemistry 2018; 2018.
19. Jeandet P, Sobarzo-Sánchez E, Uddin MS, Bru R, Clément C, Jacquard C, Nabavi SF, Khayatkashani M, Batiha GE, Khan H and Morkunas I: Resveratrol and cyclodextrins, an easy alliance: Applications in nanomedicine, green chemistry and biotechnology. Biotechnology Advances 2021; 53: 107844.
20. Dhiman P and Bhatia M: Pharmaceutical applications of cyclodextrins and their derivatives. J of Inclusion Phenomena and Macrocyclic Chem 2020; 98(3): 171-86.
21. Cheng JG, Tian BR, Huang Q, Ge HR and Wang ZZ: Resveratrol functionalized carboxymethyl-β-cyclodextrin: synthesis, characterization, and photostability. Journal of Chemistry 2018; 2018.
22. dos Santos Lima B, Shanmugam S, de Souza Siqueira Quintans J, Quintans-Junior LJ and de Souza Araujo AA: Inclusion complex with cyclodextrins enhances the bioavailability of flavonoid compounds: A systematic review. Phytochemistry Reviews 2019; 18(5): 1337-59.
23. Liu Z, Ye L, Xi J, Wang J and Feng ZG: Cyclodextrin polymers: Structure, synthesis, and use as drug carriers. Progress in Polymer Science 2021; 118: 101408.
24. Alghaith AF, Mahrous GM, Zidan DE, Alhakamy NA, Alamoudi AJ and Radwan AA: Preparation, characterization, dissolution, and permeation of flibanserin−2-HP-β-cyclodextrin inclusion complexes. Saudi Pharmaceutical Journal 2021; 29(9): 963-75.
25. Reddy MR: An Introduction to Fast Dissolving Oral Thin Film Drug Delivery Systems: A Review. Journal of Pharmaceutical Sciences and Research 2020; 12(7): 925-40.
26. Zayed GM, Abd-El Rasoul S, Ibrahim MA, Saddik MS and Alshora DH: In vitro and in vivo characterization of domperidone-loaded fast dissolving buccal films. Saudi pharmaceutical journal 2020; 28(3): 266-73.
27. Sheoran R: Fast dissolving oral films: a review with future prospects. International Journal of Pharmacy and Pharmaceutical Research 2018; 12(2): 15-32.

How to cite this article:
Shirsat VA, Hukeri AA and Govind SB: Formulation development of oral fast-dissolving sublingual film of resveratrol. Int J Pharm Sci & Res 2023; 14(5): 2447-66. doi: 10.13040/IJPSR.0975-8232.14(5).2447-66.